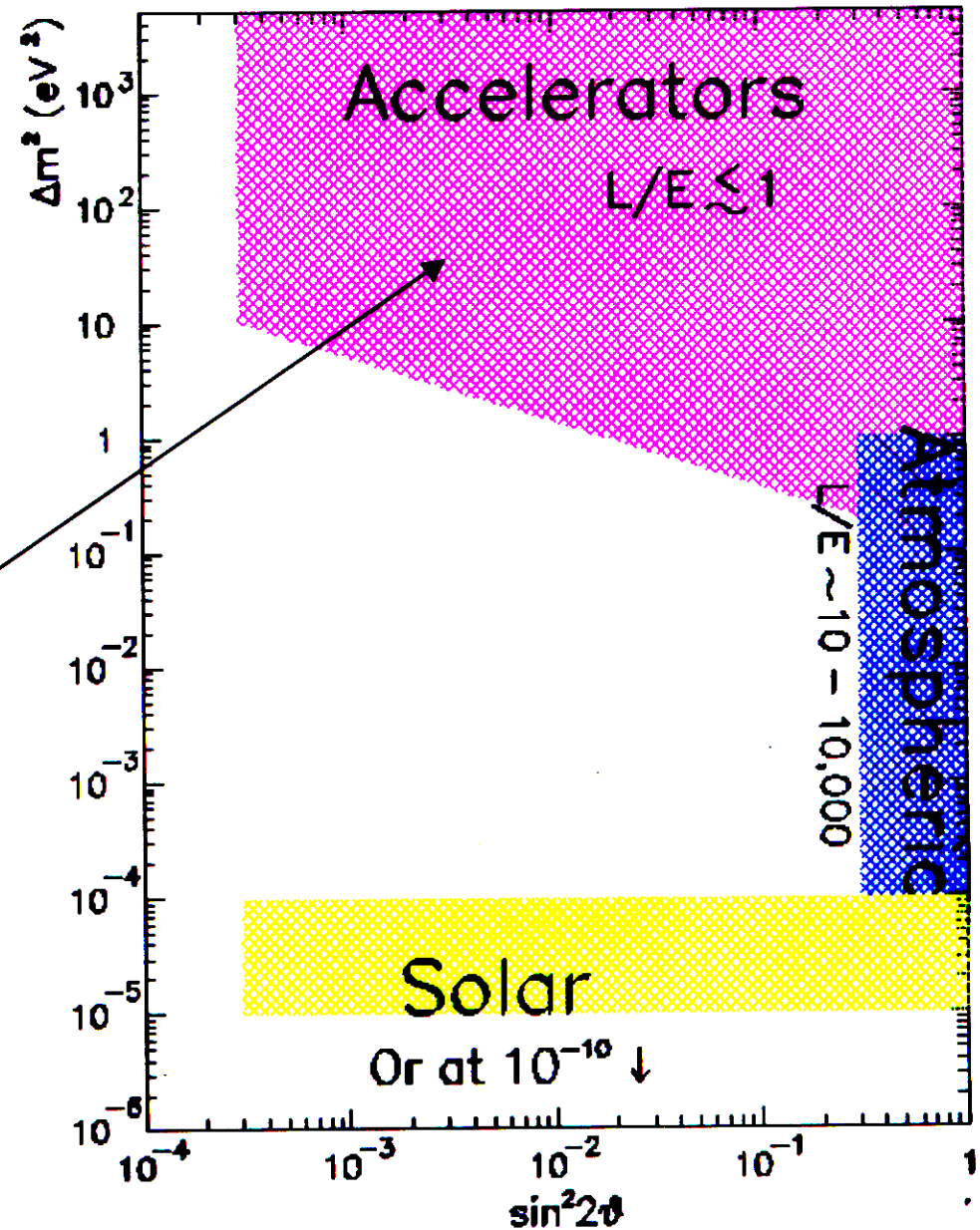


A status report on  
Investigations of  
 $\nu_\mu \rightarrow \nu_e$  at high  $\Delta m^2$

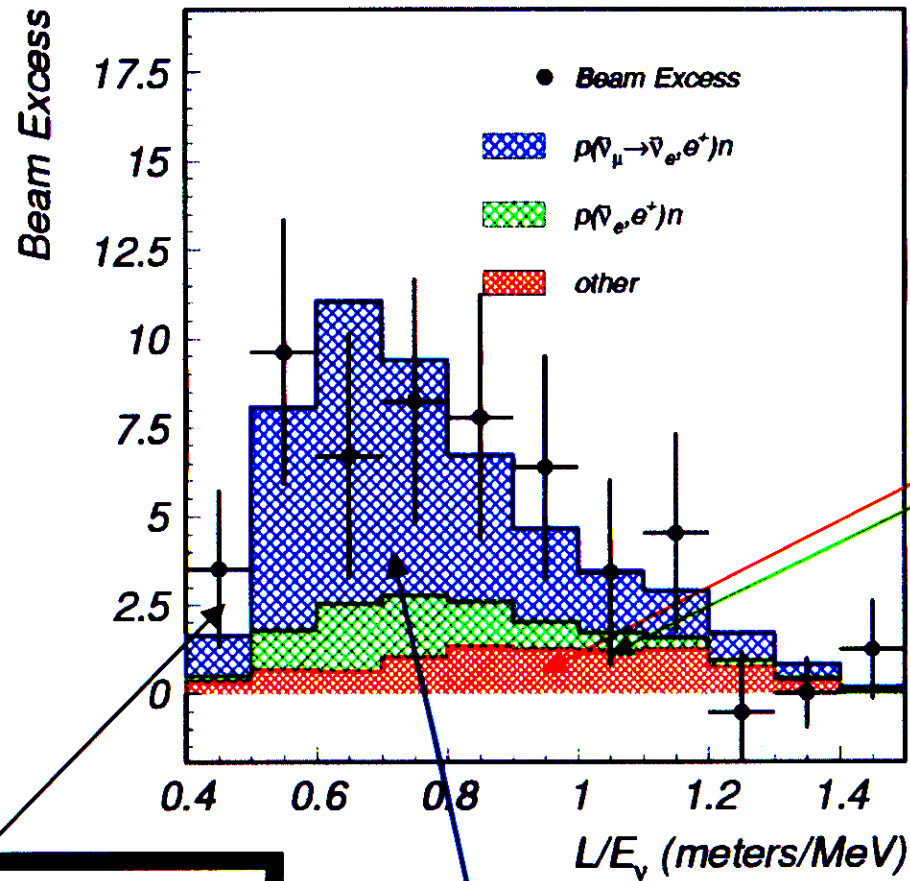
- I. LSND Final Results
- II. Karmen II Results
- III. Progress on MiniBooNE

IV. NOMAD

V. NUTEV



*The  
LSND  
DAR  
Signal*

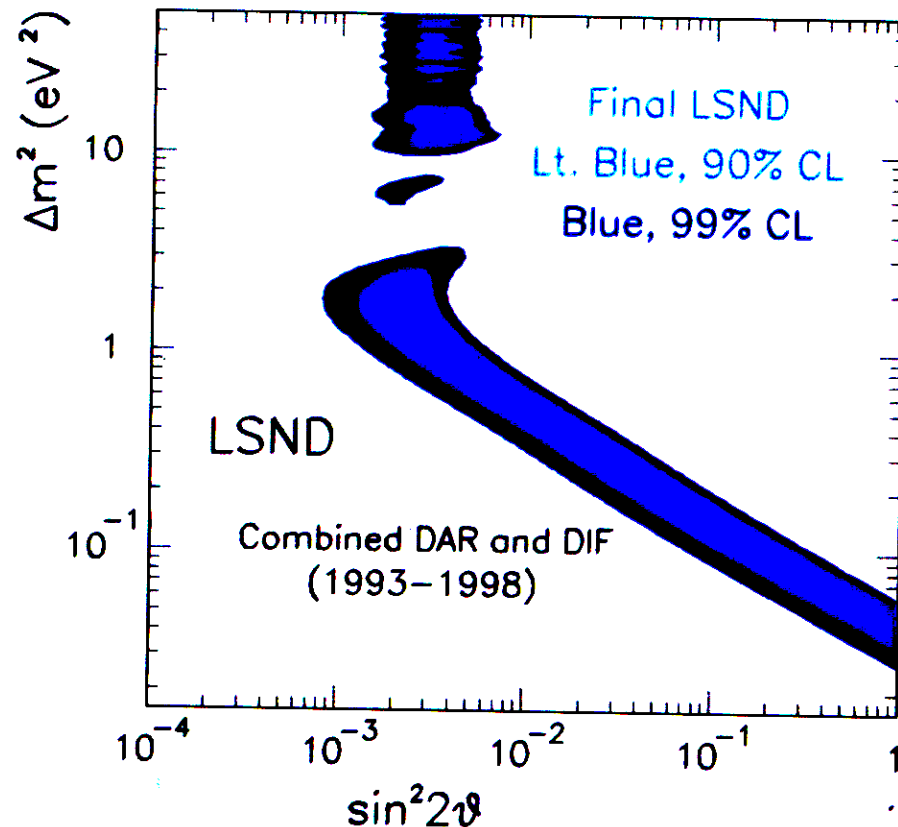


Size of the  
Beam-  
related  
backgrounds

**Data points:  
Excess after  
Beam-off  
subtraction**

**Expectation for oscillations  
(at high  $\Delta m^2$ )**

# LSND's Final Result



DAR excess:  $87.9 \pm 22.4 \pm 6.0$  evts.

Corresponding osc. probability:  
 $(0.264 \pm 0.067 \pm 0.045)\%$ .

3.3  $\sigma$  evidence for oscillation.

# We are within a few weeks of seeing Karmen II final results $(\bar{\nu}_\mu - \bar{\nu}_e)$

But not yet...

Preliminary results,

March, '00

11 events observed

$12.3 \pm 0.6$  events expected

Allows a limit of

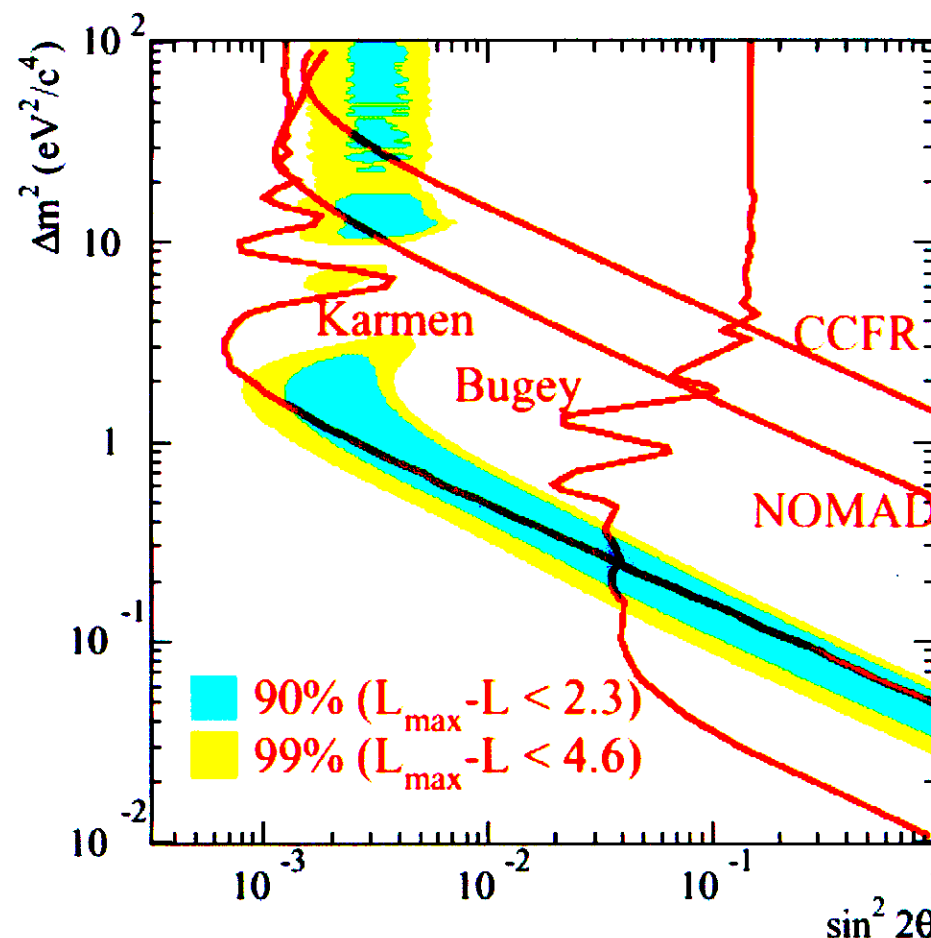
$< 3.1$  oscillation events

In the Karmen II data @ 90% CL

(Announced at Karmenfest:

Results through Nov '00:

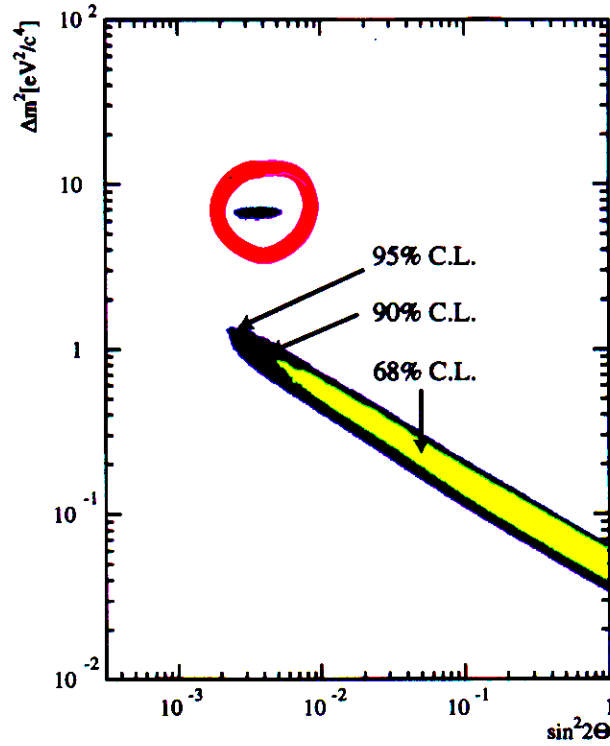
14 observed, 14.3 expected)



*Also coming soon: A new joint analysis by Klaus Eitel!*

# UNIFIED APPROACH

LSND  
+  
KARMEN 2  
joint  
analysis



$\bar{\nu}_\mu - \bar{\nu}_e$

FIG. 9: Regions of various confidence for the combined analysis assuming statistical compatibility of KARMEN 2 and LSND.

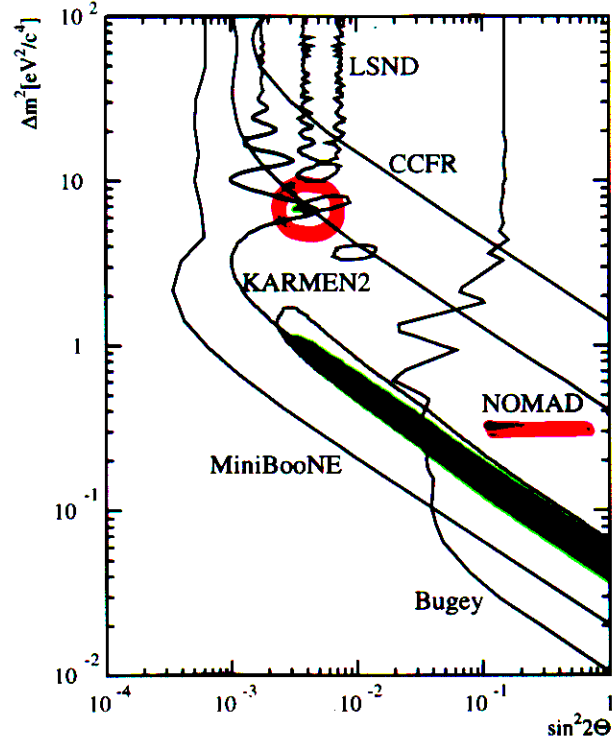
to the no-oscillation value is reduced (see Equ. 2.7) as well as the shape at higher values of  $\Delta m^2$  is significantly modified due to the KARMEN 2 likelihood function.

To determine the confidence regions in  $(\sin^2(2\theta), \Delta m^2)$ , again we apply the unified approach, i.e. we create the estimator distribution  $\Delta \ln \mathcal{L}_{K+L}$  for various hypotheses  $(\sin^2(2\theta), \Delta m^2)_H$  and compare the experiment's value  $\Delta \ln \mathcal{L}_{KARMEN2+LSND}$  with the cut value  $\Delta \ln \mathcal{L}_{K+L}(\delta)$  for a given confidence. To get the estimator, a simulated event sample now consists of a KARMEN 2-like and an LSND-like MC sample each analysed with the appropriate likelihood definitions. Then both likelihood functions are added following equation (4.2) and the estimator  $\Delta \ln \mathcal{L}_{K+L} = \ln \mathcal{L}_{K+L}(\sin^2(2\theta), \Delta m^2)_{max} - \ln \mathcal{L}_{K+L}(\sin^2(2\theta), \Delta m^2)_H$  is calculated. The typical cut values for a confidence of  $\delta = 90\%$  are slightly higher than the individual LSND ones, ranging from 3.5 to 5.5. Figure 9 shows the confidence regions of the oscillation parameters for the combined likelihood analysis. The total confidence of a parameter region is hereby reduced by the fraction of incompatibility

K. Eitel et al.

Assume CP cons

$$P(\nu_\mu \rightarrow \nu_e) = P(\bar{\nu}_\mu \rightarrow \bar{\nu}_e)$$



EPS 01  
 $\nu_\mu - \nu_e$

FIG. 10: Parameter regions deduced in this work (grey area) compared with existing limits of experiments (Bugey  $\bar{\nu}_e \rightarrow \bar{\nu}_\mu$  [18], CCFR  $\nu_\mu \rightarrow \nu_e$  [19] and NOMAD  $\nu_\mu \rightarrow \nu_e$  [20]) and the envisaged sensitivity of the MiniBooNE experiment (with final single horn design [21]).

applied a unified frequentist approach to both likelihood analyses individually. The results underline the feasibility of as well as the necessity for such an approach.

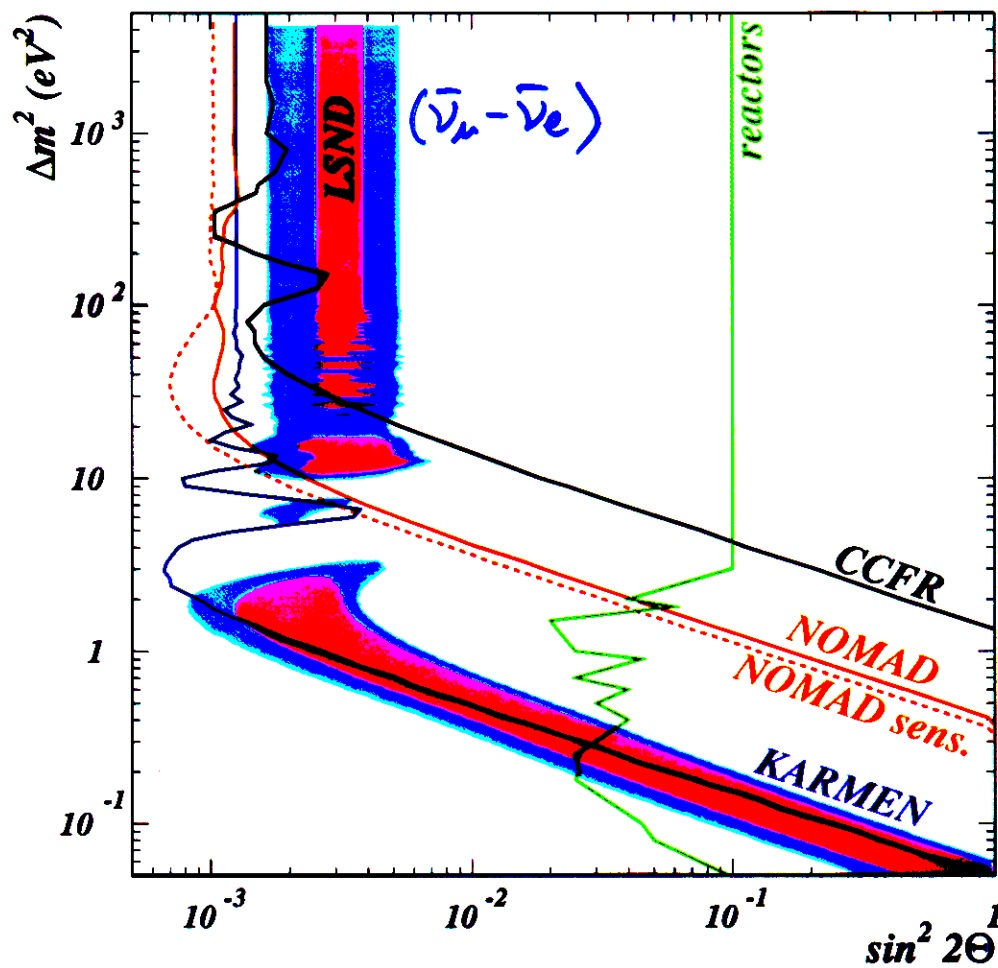
A quantitative joint statistical analysis has been performed leading to a level of 36 % incompatibility of the experimental outcomes, corresponding to individual confidence levels of 60 %. For the cases of statistical compatibility, the common parameter regions have been identified on the basis of the unified frequentist approach applied to the combined likelihood function of KARMEN 2 and LSND. The derived confidence regions in  $(\sin^2(2\Theta), \Delta m^2)$  clearly differ from an often applied but incorrect graphical overlap of the confidence regions of the individual experiments. There are two oscillation scenarios with either  $\Delta m^2 \approx 7 \text{ eV}^2/\text{c}^4$  or  $\Delta m^2 < 1 \text{ eV}^2/\text{c}^4$  compatible with both experiments.

We performed a joint statistical analysis incorporating some of the systematic uncertainties of the experiments, such as neutrino flux uncertainty, accuracy of known cross sections and resolution functions of both experiments. Further –unknown– systematic uncertainties

# EPS01 - NOMAD

## Exclusion Region (Preliminary)

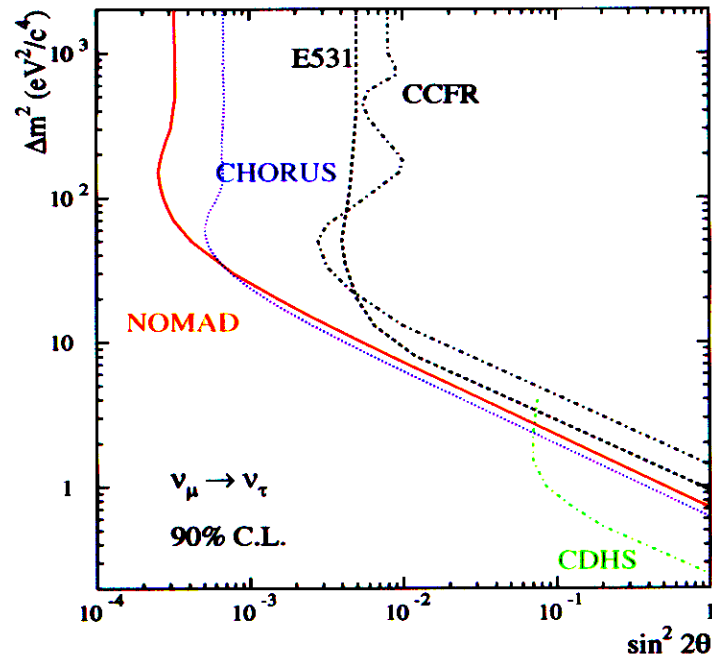
(full NOMAD data sample)



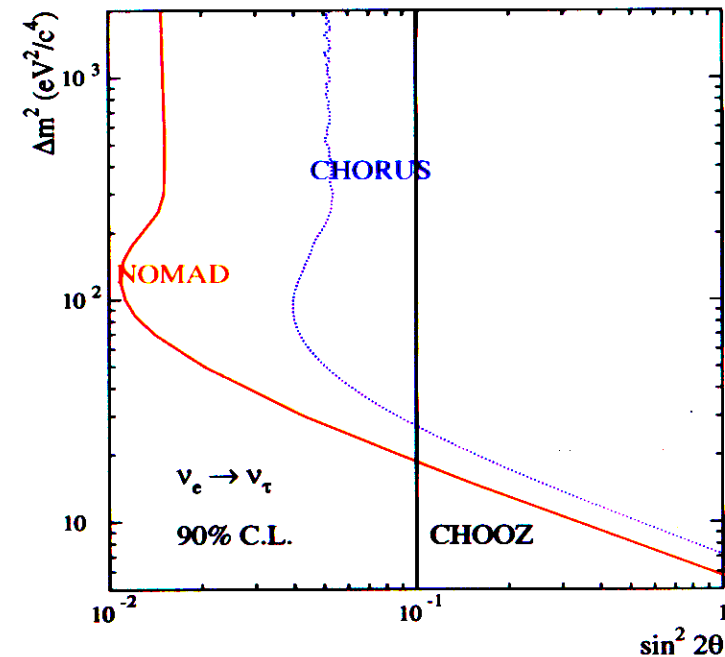
At large  $\Delta m^2$ :  $\sin^2 2\theta < 1.2 \times 10^{-3}$  @ 90% C.L.  
(Feldman-Cousins method)

# Final Results of the $\nu_\tau$ Search

•  $\nu_\mu \rightarrow \nu_\tau$



•  $\nu_e \rightarrow \nu_\tau$



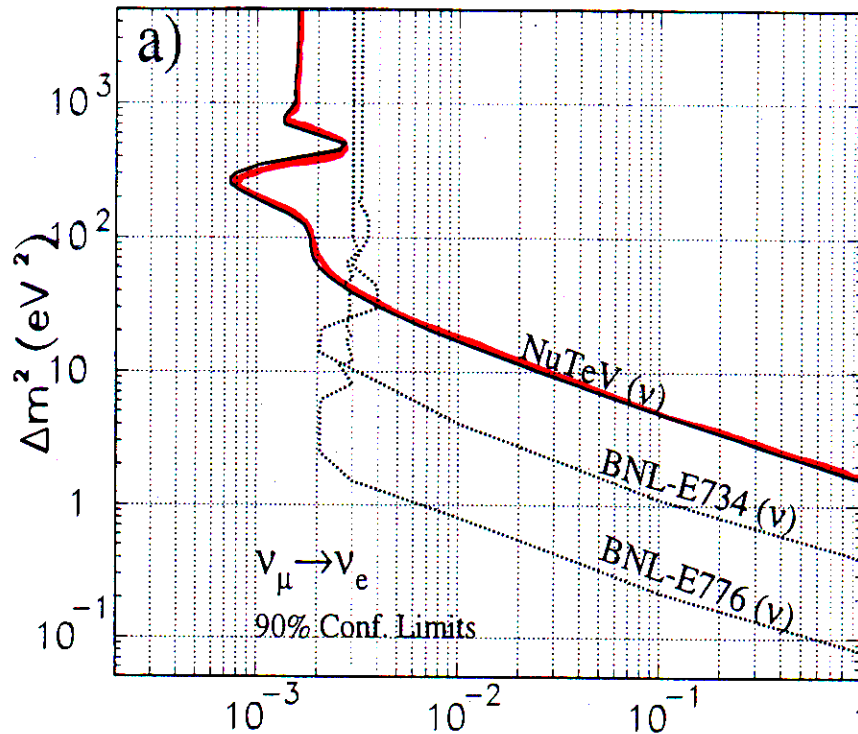
$$\begin{cases} S_{\nu_\mu \rightarrow \nu_\tau} &= 2.50 \times 10^{-4} \\ L_{\nu_\mu \rightarrow \nu_\tau} &= 1.63 \times 10^{-4} \quad (90\% \text{ C.L.}) \\ P(\leq L) &= 37\% \end{cases}$$

$$\begin{cases} S_{\nu_e \rightarrow \nu_\tau} &= 1.10 \times 10^{-2} \\ L_{\nu_e \rightarrow \nu_\tau} &= 0.74 \times 10^{-2} \\ P(\leq L) &= 39\% \end{cases}$$

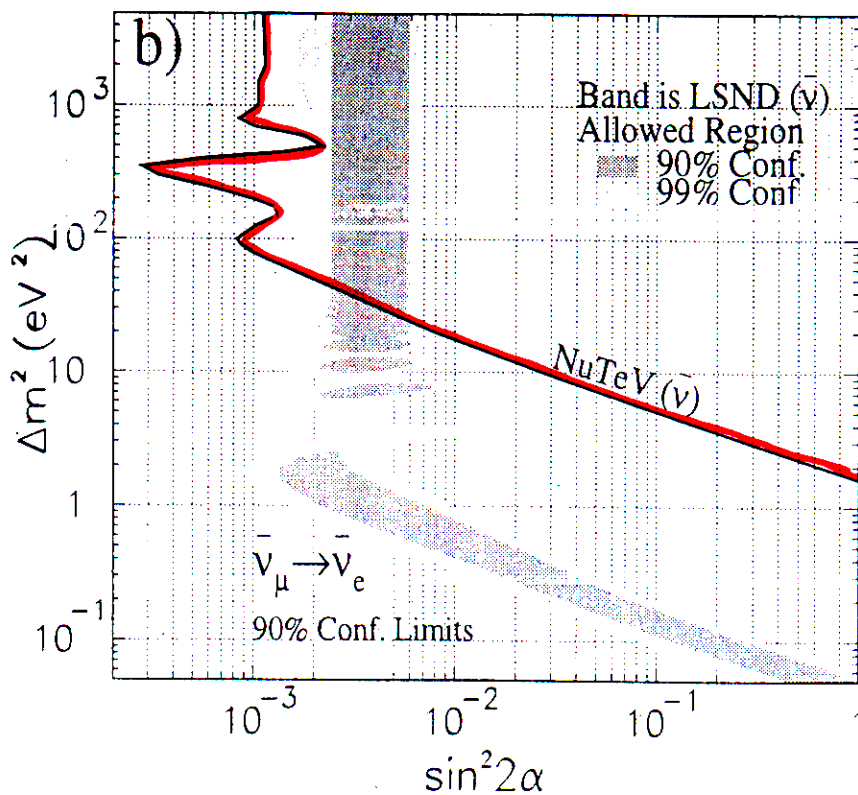


# NuTeV

hep-ex/0203018



$\nu_\mu - \nu_e$



$\bar{\nu}_\mu - \bar{\nu}_e$

N.B. 1) RASTER SCAN  $\Leftarrow$  bad coverage

2) LIMIT obtained from gaussian centered in UNPHYSICAL REGION ( $\sin^2 2\theta_{\text{best}} < 0$ !)

# INTERPRETATION of ALL $\vee$ DATA

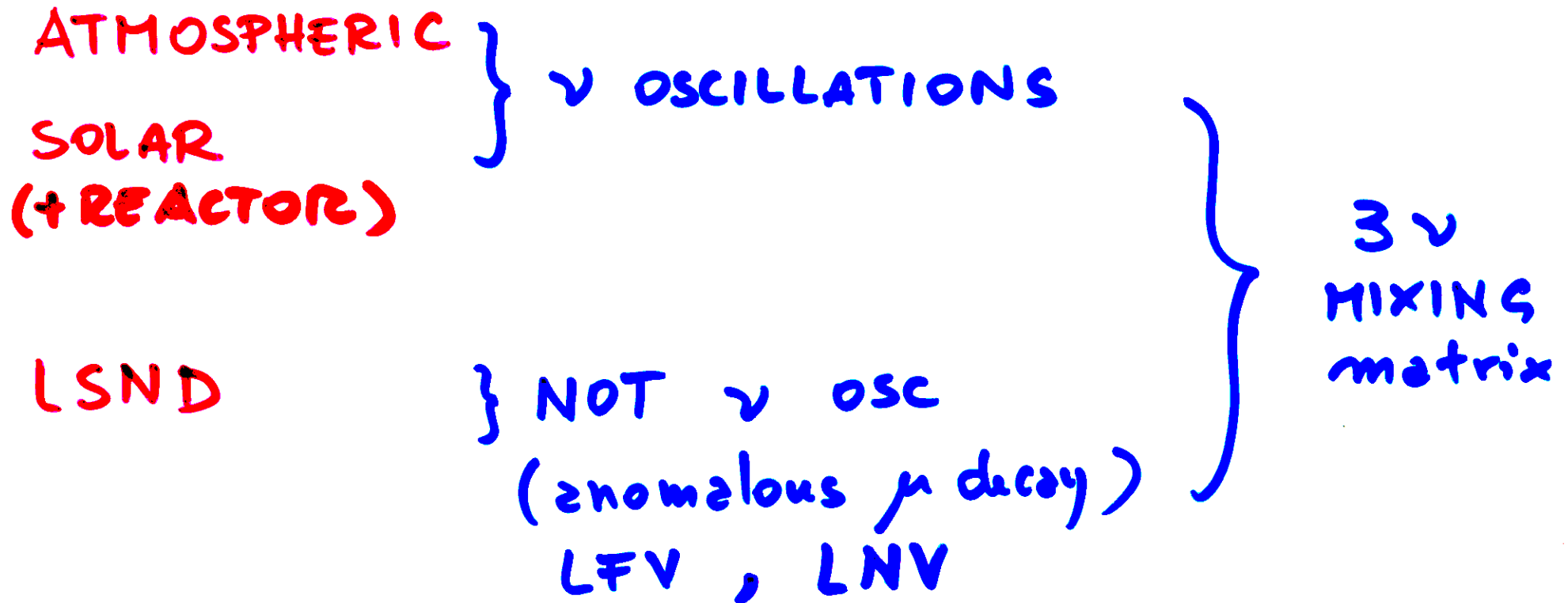
## SECOND PART

### NON STANDARD SCENARIOS

- \* in evolution
- \* experiment - driven

# Interpretations of $\nu$ DATA - ①

## SECOND PART



In this case  $\nu$  mass is not relevant for cosmology  
(unit scale is  $\text{meV}$ )

# The flavor of neutrinos in muon decays at a neutrino factory and the LSND puzzle

---

**Antonio Bueno, Mario Campanelli, Javier Rico and André Rubbia**

*Institut für Teilchenphysik, ETHZ, CH-8093 Zürich, Switzerland*

*E-mail: Antonio.Bueno@cern.ch, Mario.Campanelli@cern.ch,*

*Javier.Rico@cern.ch, Andre.Rubbia@cern.ch*

**Marco Laveder**

*Dipartimento di Fisica "G. Galilei"*

*Università di Padova, and*

*INFN Sez. di Padova*

*I-35131 Padova, Italy*

*E-mail: Marco.Laveder@pd.infn.it*

**ABSTRACT:** The accurate prediction of the neutrino beam produced in muon decays and the absence of opposite helicity contamination for a particular neutrino flavor make a future neutrino factory the ideal place to look for the lepton flavor violating (LFV) decays of the kind  $\mu^+ \rightarrow e^+ \bar{\nu}_e \nu_\mu$  and lepton number violating (LNV) processes like  $\mu^- \rightarrow e^- \nu_e \nu_\mu$ . Excellent sensitivities can be achieved using a detector capable of muon and/or electron identification with charge discrimination. This would allow to set experimental limits that improve current ones by more than two orders of magnitude and test the hypothesis that the LSND excess is due to such anomalous decays, rather than neutrino flavor oscillations in vacuum.

**KEYWORDS:** Beyond Standard Model, Neutrino Physics, Rare Decays.

decay

interaction

● Standard  $\mu^+ \rightarrow e^+ \nu_e \bar{\nu}_\mu$

$$\nu_e N \rightarrow e^- X$$

$$\bar{\nu}_\mu N \rightarrow \mu^+ X$$

● LFV  $\mu^+ \rightarrow e^+ \bar{\nu}_e \nu_\mu$

$$\bar{\nu}_e N \rightarrow e^+$$

$$\nu_\mu N \rightarrow \mu^- \quad \text{WRONG SIGN } \mu$$

MUON DETECTOR with charge id

● LNV  $\mu^+ \rightarrow e^+ \bar{\nu}_\mu \bar{\nu}_e$

$$\bar{\nu}_\mu N \rightarrow \mu^+$$

$$\bar{\nu}_e N \rightarrow e^+ \quad \text{WRONG SIGN } e$$

$$(\mu^- \rightarrow e^- \nu_\mu \nu_e)$$

more convenient

DETECTOR with e charge discr.!!!

# SIGNAL

LFV:

$$\mu^+ \rightarrow e^+ \nu_e (\nu_\mu)$$

$$\nu_\mu N \rightarrow \mu^- X$$

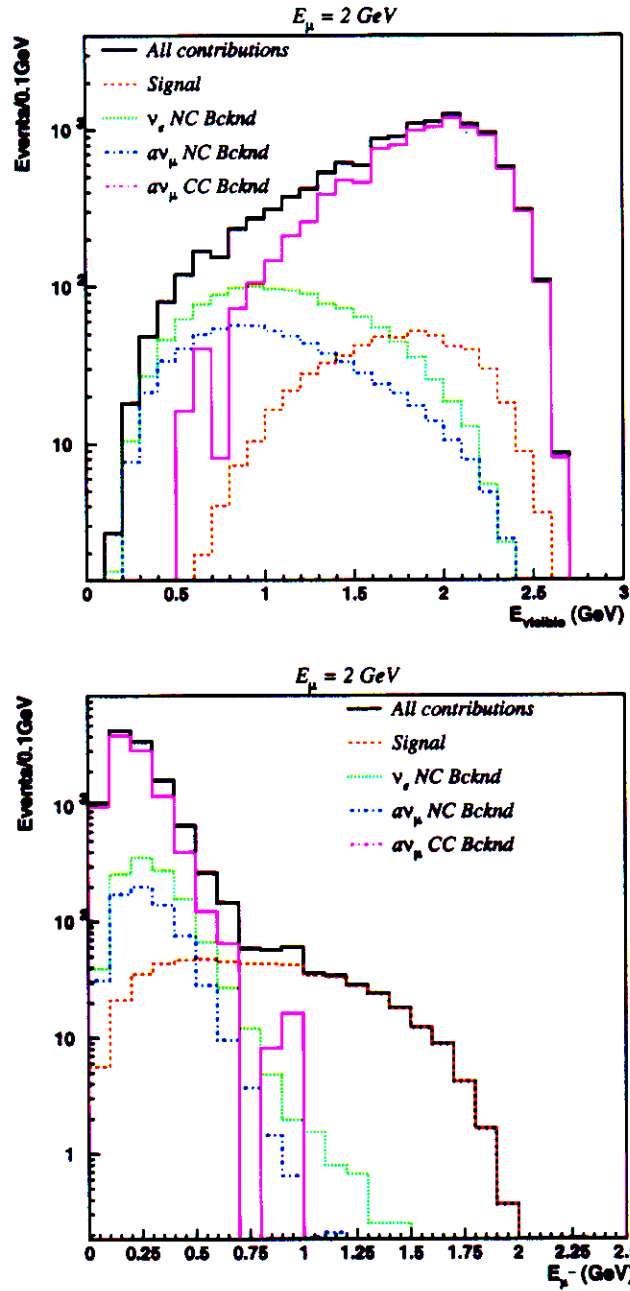


**Figure 3:** Visible energy (upper) and candidate muon (lower) distribution for LFV decays (see text) normalized to LSND excess and  $10^{19}$  positive muon decays for 10 ton detector. The background from neutral current using the characteristics of an ICARUS LAr TPC is also shown.

energy distribution with the help of an event generator [38] which includes all exclusive final states and a realistic treatment of the low energy region.

A muon candidate is identified as a track which stops without interacting in the Argon or leaves the detector vessel before interacting or stopping. Hence, **charged**

JHEP06(2001)032

# LIMITS

$\mu$ Decays	Decay mode	Current direct Limit	$E_\mu = 1 \text{ GeV}$	$E_\mu = 2 \text{ GeV}$	$E_\mu = 5 \text{ GeV}$
$10^{18}$	$P(\mu^+ \rightarrow e^+ \bar{\nu}_\ell \nu_\mu) <$	$1.2 \times 10^{-2}$	$4 \times 10^{-3}$	$5 \times 10^{-4}$	$1 \times 10^{-4}$
$10^{19}$			$5 \times 10^{-4}$	$1 \times 10^{-4}$	$3 \times 10^{-5}$
$10^{20}$			$2 \times 10^{-4}$	$6 \times 10^{-5}$	$2 \times 10^{-5}$
$10^{18}$	$P(\mu^- \rightarrow e^- \nu_e \nu_\ell) <$	—	$6 \times 10^{-3}$	$3 \times 10^{-3}$	$9 \times 10^{-4}$
$10^{19}$			$6 \times 10^{-4}$	$3 \times 10^{-4}$	$3 \times 10^{-4}$
$10^{20}$			$1 \times 10^{-4}$	$1 \times 10^{-4}$	$2 \times 10^{-4}$

Table 4: Achievable limits in case of negative result at the 90% C.L. for  $\mu^+ \rightarrow e^+ \bar{\nu}_\ell \nu_\mu$  and  $\mu^- \rightarrow e^- \nu_e \nu_\ell$  decays with a 10 ton detector for three different number of muon decays. For comparison, the indirect limit obtained in ref. [30] using processes involving charged leptons is  $5.8 \times 10^{-4}$ .

In particular, LFV and LVN decays could play a role in the interpretation of the LSND excess. Theoretical arguments based on experimental limits obtained on exotic charged lepton decays, indicate that most probably the LSND excess cannot be explained by these processes. However, if the LSND puzzle remains unsolved after the MiniBOONE [28] results, a better understanding of these processes would then be particularly relevant, if not mandatory.

A neutrino factory is an ideal machine to probe such anomalous decays of the muon. The pure initial state beam allows to look for these decays without intrinsic beam contamination.

## References

- [1] P. Herczeg, *The Neutrinos in muon decay*, *Z. Physik C* **56** (1992) S129.
- [2] P. Herczeg, *The nature of neutrinos in muon decay and physics beyond the standard model*, Los Alamos Sci. 1997 No. 25 pp. 128–135.
- [3] MEGA collaboration, *New limit for the family-number non-conserving decay  $\mu^+ \rightarrow e^+ \gamma$* , *Phys. Rev. Lett.* **83** (1999) 1521 [[hep-ex/9905013](#)].
- [4] U. Bellgardt et al., *search for the decay  $\mu^+ \rightarrow e^+ e^+ e^-$* , *Nucl. Phys. B* **299** (1988) 1.
- [5] P. Wintz, *Results of the SINDRUM II experiment*, in *Proceedings of the first international symposium on lepton and baryon number violation*, H.V. Klapdor-Kleingrothaus and I.V. Krivosheina eds., Institute of Physics, Bristol 1998, p. 534.
- [6] CLEO collaboration, *Update of the search for the neutrinoless decay  $\tau \rightarrow \mu \gamma$* , *Phys. Rev. D* **61** (2000) 071101 [[hep-ex/9910060](#)].
- [7] P. Herczeg, *Lepton family number violation*, in *Proceedings of the Zuoz summer school on hidden symmetries and Higgs phenomena*, Zuoz, Switzerland, 16–22 Aug. 1998.

# Interpretations of $\nu$ DATA - ②

## SECOND PART

ATMOSPHERIC	}	FLAVOR $\nu$ OSCILLATIONS 3 different $\Delta m^2$	{	4 $\nu$ MIXING (3 active + 1 sterile)
SOLAR				
LSND				
(+REACTOR)				

Missing:  $0\nu 2\beta$  evidence (?)  
 (2002) NUTEV  $\nu_e - \nu_s$  disappearance (?)



# Sterile Neutrino

- $\nu_{\mu}$ , atmospheric and solar neutrino oscillation signals

$$\Delta m^2_{\text{LSND}} \sim \text{eV}^2$$

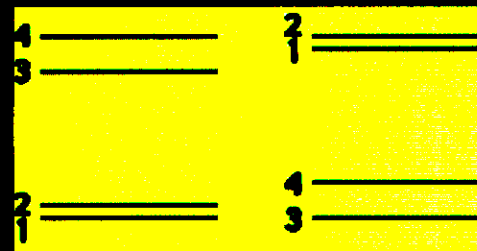
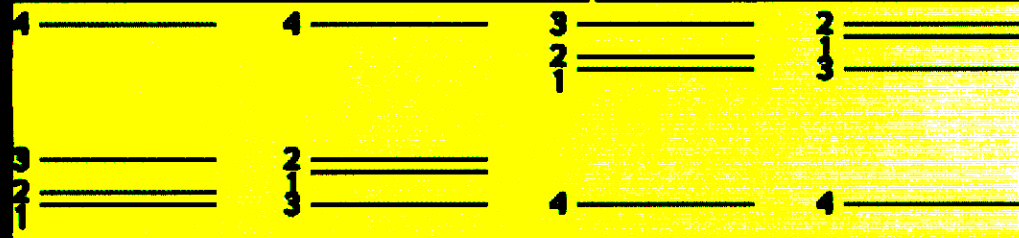
$$\Delta m^2_{\text{atm}} \sim 3 \times 10^{-3} \text{eV}^2$$

$$\Delta m^2_{\text{solar}} < 10^{-3} \text{eV}^2$$

$\Rightarrow$  Can't be accommodated with 3 neutrinos

$\Rightarrow$  Need a sterile neutrino

- 3+1 or 2+2 spectrum?



## But Not Excluded Yet!

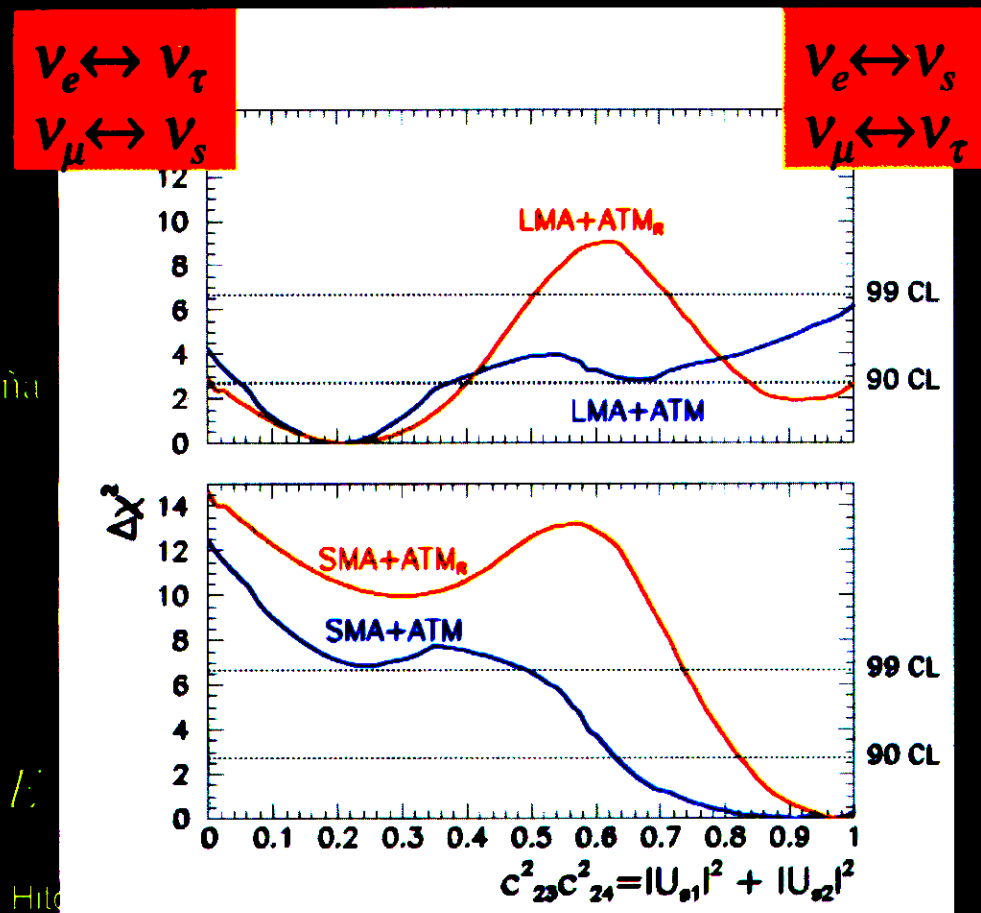
- Global fit to four-neutrino oscillation

Solar, Atmospheric,  
LSND

(Gonzalez-Garcia, Maltoni, Peña  
Garay & EPS01)

- One can still find a reasonable fit with  $2+2$

$\Rightarrow$  Wait for MiniBooNE



# Large $\nu_\mu \rightarrow \nu_\tau$ and $\nu_e \rightarrow \nu_\tau$ transitions in short-baseline experiments?

---

**Carlo Giunti**

*INFN, Sezione di Torino, and  
Dipartimento di Fisica Teorica, Università di Torino  
I-10125 Torino, Italy, and  
School of Physics, Korea Institute for Advanced Study  
Seoul 130-012, Korea  
E-mail: giunti@to.infn.it*

**Marco Laveder**

*Dipartimento di Fisica "G. Galilei", Università di Padova, and  
INFN, Sezione di Padova  
I-35131 Padova, Italy  
E-mail: marco.laveder@pd.infn.it*

with  $|U_{\mu 4}|^2 \ll 1$

**ABSTRACT:** Considering four-neutrino schemes of type  $3 + 1$ , we identify four small regions of the neutrino mixing parameter space compatible with all data. Assuming a small mixing between the sterile neutrino and the isolated mass eigenstate we show that large  $\nu_\mu \rightarrow \nu_\tau$  and  $\nu_e \rightarrow \nu_\tau$  transitions are predicted in short-baseline experiments and could be observed in the near future in dedicated experiments. We discuss also implications for solar, atmospheric and long-baseline neutrino experiments and we present a formalism that allows to describe in  $3 + 1$  schemes atmospheric neutrino oscillations, long-baseline  $\nu_\mu$  disappearance and  $\nu_\mu \rightarrow \nu_\tau$  transitions in matter.

**KEYWORDS:** Solar and Atmospheric Neutrinos, Neutrino Physics.

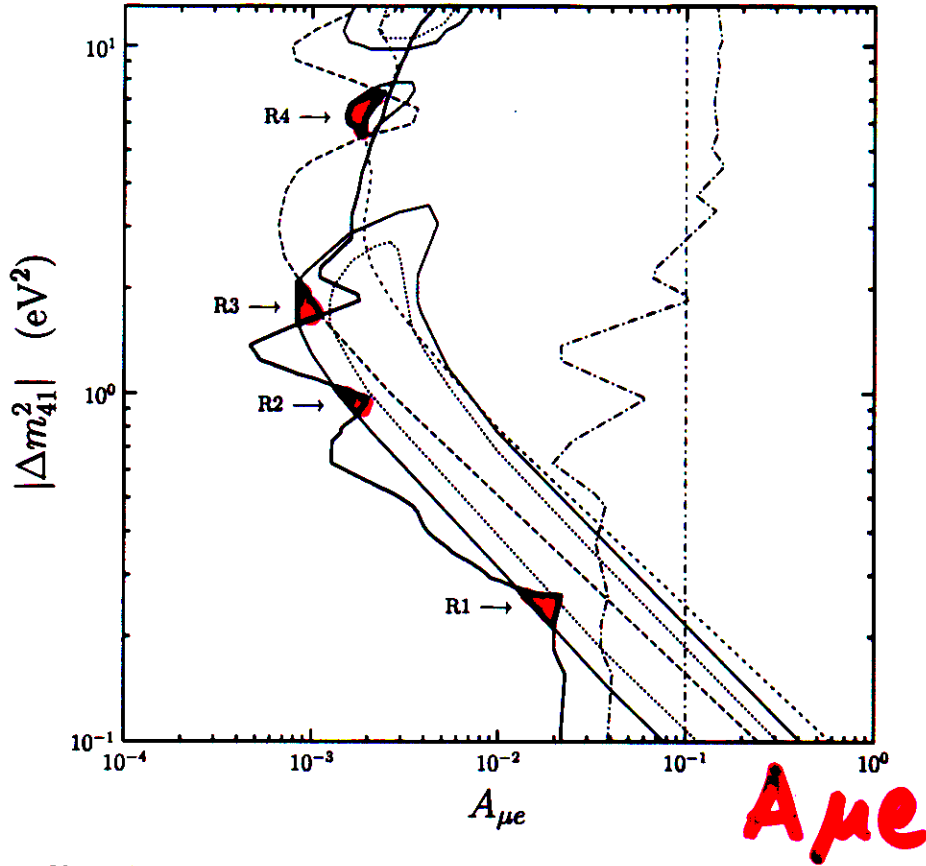
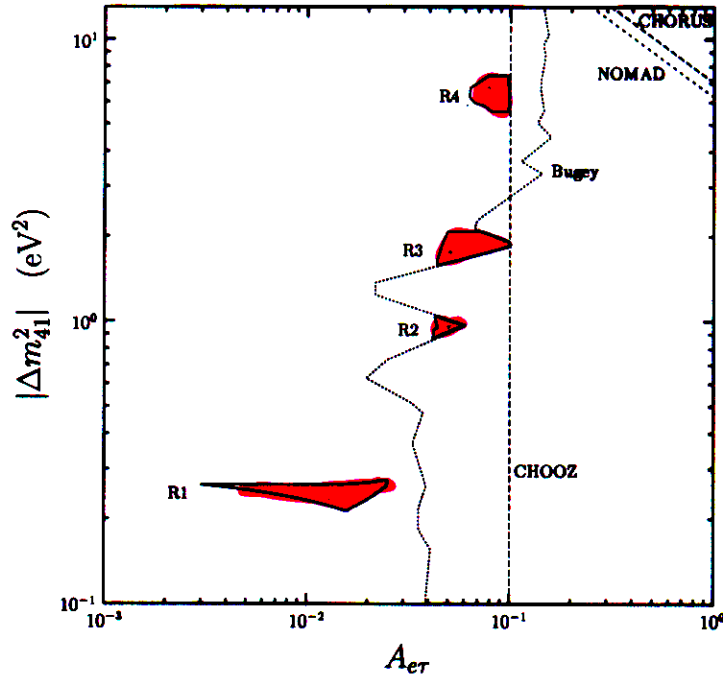


**Figure 2:** *Very Thick Solid Line:* Allowed regions. *Thick Solid Line:* Disappearance bound (3.5). *Dotted Line:* LSND 2000 allowed regions at 90% CL [31]. *Solid Line:* LSND 2000 allowed regions at 99% CL [31]. *Broken Dash-Dotted Line:* Bugey exclusion curve at 90% CL [32]. *Vertical Dash-Dotted Line:* CHOOZ exclusion curve at 90% CL [23]. *Long-Dashed Line:* KARMEN 2000 exclusion curve at 90% CL [36]. *Short-Dashed Line:* BNL-E776 exclusion curve at 90% CL [35].

that could be observed in the near future. We consider the 3 + 1 schemes with

$$|U_{s4}|^2 \ll 1. \quad (1.3)$$

This could be obtained, for example, in the hierarchical scheme I (see figure 1) with an appropriate symmetry keeping the sterile neutrino very light, i.e. mostly mixed with the lightest mass eigenstates. Notice that nothing forbids  $|U_{s4}|^2$  to be even zero exactly. The only unwelcomed consequence of equation (1.3) is a large contribution of  $\nu_\mu \rightarrow \nu_s$  transitions to the atmospheric neutrino anomaly, as discussed in section 4. These transitions are dominant in the regions R2, R3, R4, whereas they mix with  $\nu_\mu \rightarrow \nu_\tau$  transitions in the region R1. As mentioned above, dominant  $\nu_\mu \rightarrow \nu_s$  transitions of atmospheric neutrinos are disfavored by the present Super-Kamiokande and MACRO data [20, 22]. On the other hand, a mixture of  $\nu_\mu \rightarrow \nu_s$  and  $\nu_\mu \rightarrow \nu_\tau$  transitions is allowed by the data [49, 51, 52].



A<sub>e</sub>τ

**Figure 8:** *Solid Line:* Allowed regions. *Long Dashed Line:* CHORUS exclusion curve at 90% CL [37]. *Short Dashed Line:* NOMAD exclusion curve at 90% CL [38]. *Dotted Line:* Bugey exclusion curve at 90% CL [32]. *Dashed Line:* CHOOZ exclusion curve at 90% CL [23].

2.  $|U_{\mu 4}|^2 \simeq 0.33 - 0.55$  in region R1 in figure 4. In this case the solar neutrino problem is due to a mixture of  $\nu_e \rightarrow \nu_\mu$ ,  $\nu_e \rightarrow \nu_\tau$  and  $\nu_e \rightarrow \nu_s$  transitions, that is allowed by data as in the previous case.

The atmospheric neutrino anomaly is due to a mixture of  $\nu_\mu \rightarrow \nu_\tau$  and  $\nu_\mu \rightarrow \nu_s$  transitions. In refs. [49, 51, 52] it has been shown that a mixture of  $\nu_\mu \rightarrow \nu_\tau$  and  $\nu_\mu \rightarrow \nu_s$  transitions in the framework of  $2 + 2$  schemes is allowed by the atmospheric neutrino data. This indicates that such a mixture should be allowed also in the framework of  $3 + 1$  schemes. The groups specialized in the analysis of atmospheric neutrino data could check this possibility using the formalism presented in appendix A. The existence of mixed  $\nu_\mu \rightarrow \nu_\tau$  and  $\nu_\mu \rightarrow \nu_s$  transitions can also be checked by comparing the rates of  $\nu_\mu$  disappearance and  $\nu_\mu \rightarrow \nu_\tau$  appearance in future long-baseline experiments with  $\nu_\mu$  beams. The formalism that allows to describe these oscillation channels in the framework of  $3 + 1$  four-neutrino schemes is presented in appendix A.

These predictions are testable in future experiments, especially measuring the percentage of transitions into active and sterile neutrinos in solar, atmospheric and long-baseline experiments (that should measure the same transitions observed in

# hep-ph/0112103 v3

$\eta_s \equiv$  fraction of sterile in solar  $\nu$

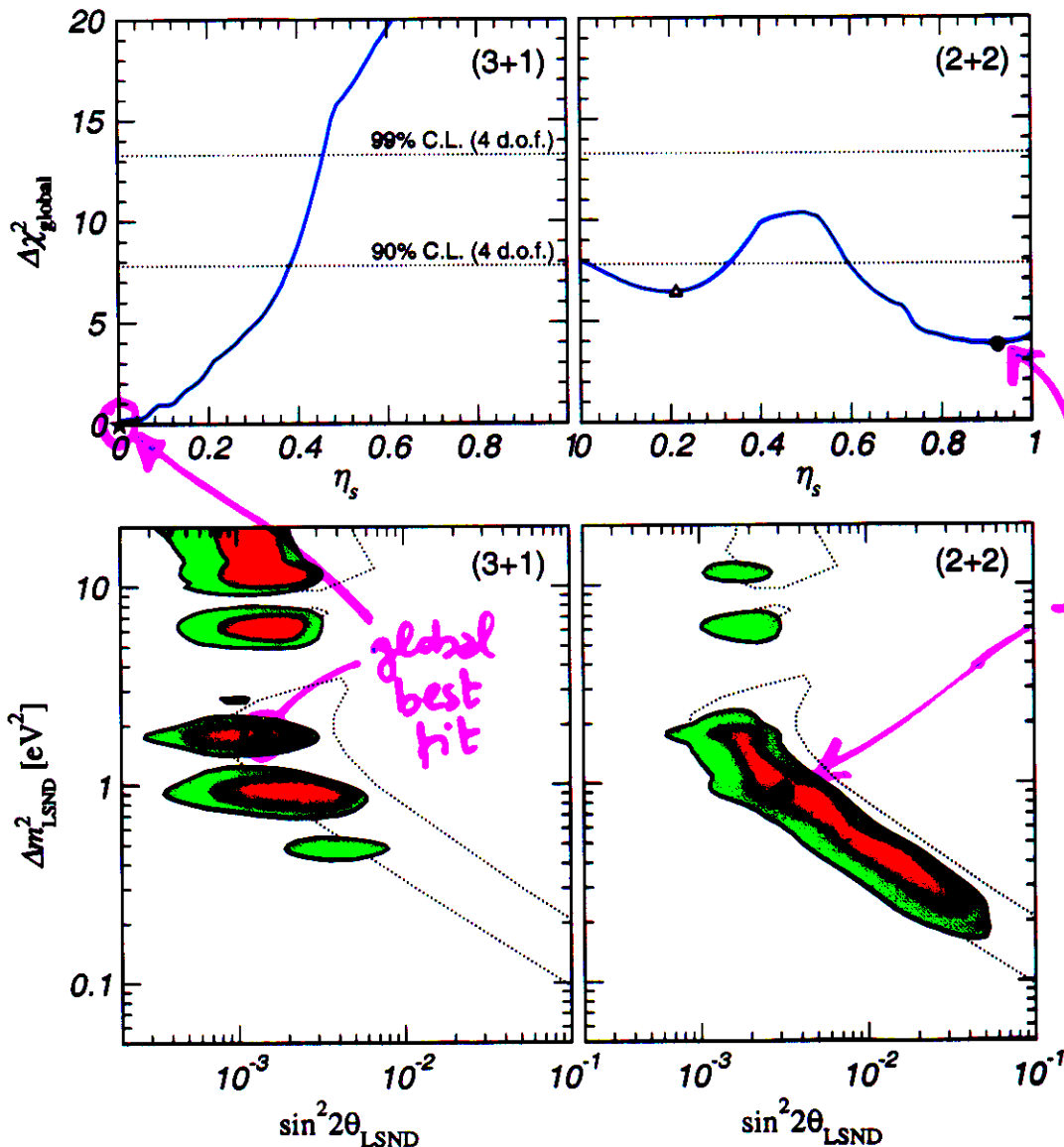


Figure 8: Global combination of current neutrino oscillation data: solar, atmospheric and SBL. We show the  $\Delta\chi^2_{\text{global}}$  as a function of  $\eta_s$  (upper panels) and projections of the four-dimensional 90% and 99% C.L. regions on the  $(\Delta m^2_{\text{LSND}}, \sin^2 2\theta_{\text{LSND}})$  plane (lower panels) (see text for details). The global best fit point lies in (3+1) and is marked with a star, the local best fit point in (2+2) is marked with a circle and the local minimum in (2+2) is marked with a triangle. The dotted line in the lower panels is the 99% C.L. region from LSND data alone [11].

four-dimensional volumes onto the  $(\Delta m^2_{\text{LSND}}, \sin^2 2\theta_{\text{LSND}})$  plane. In the upper panels we show  $\Delta\chi^2_{\text{global}}$  minimized with respect to all parameters except  $\eta_s$ . The projections of the four-dimensional 90% and 99% C.L. volumes onto the  $\eta_s$ -axis are given by the intersections of the solid lines in the upper panels with the corresponding horizontal dotted lines.

Let us discuss the results of the global analysis. We find that the global minimum lies in

VALENCIA group - feb 2002

# Interpretation of $\nu$ DATA - ③

## SECOND PART

ATM  
SOLAR  
LSND  
(+ REACTOR)

FLAVOR  
 $\nu$  OSCILLATION  
3 different  $\Delta m^2$

~~CPT~~  
 $\nu$  &  $\bar{\nu}$   
MIXING  
6 mass  
eigenstates  
(3 +  $\bar{3}$ )

- CPT violation is extremely strong request!



Figure 2: Typical  $CPT$  violating (hierarchical) spectrum, able to account for the LSND, atmospheric and solar neutrino evidence



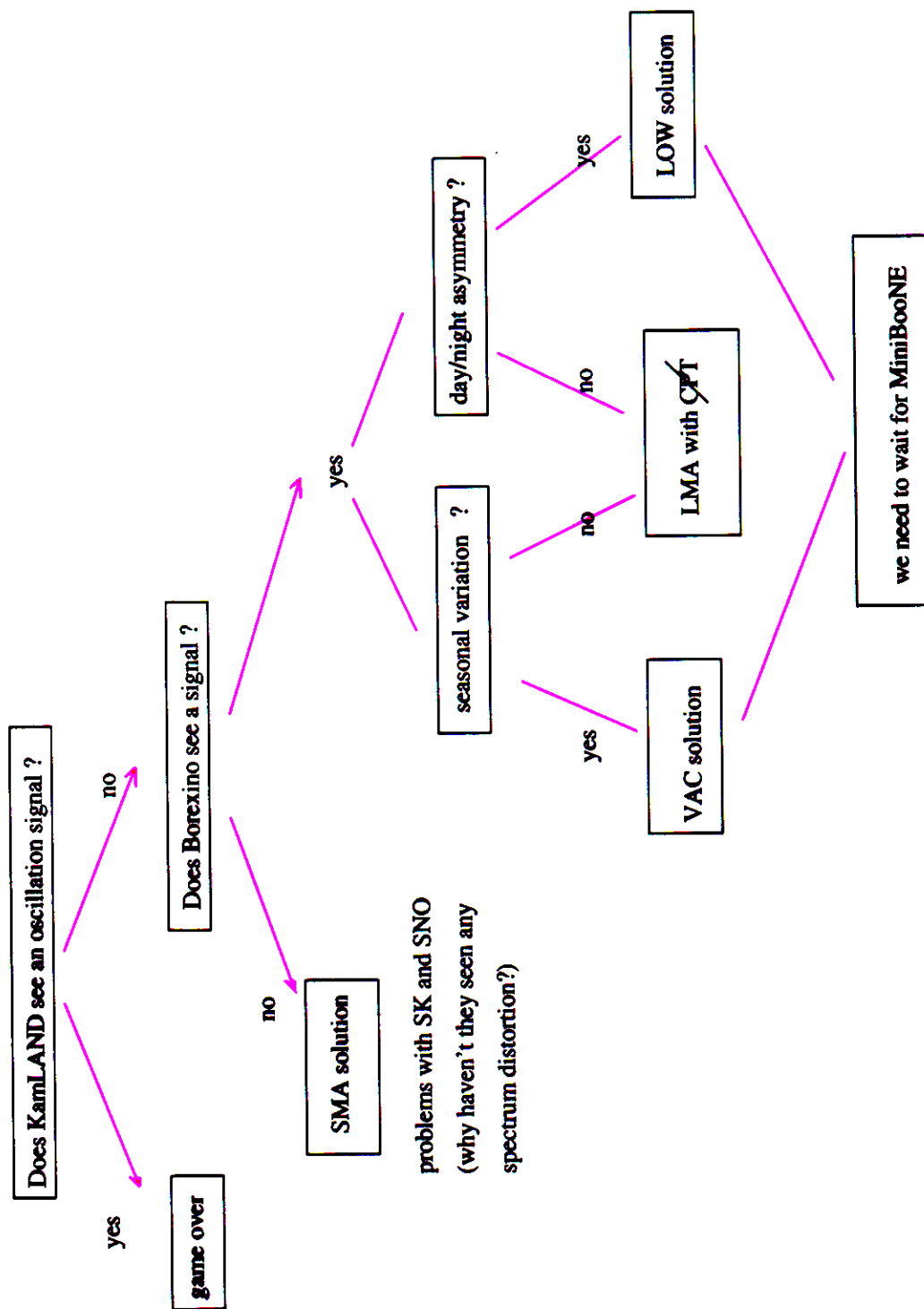


Figure 1: Flow chart for discovering  $CPT$  violation by combining the results of KamLAND and Borexino

hep-ph/0201080

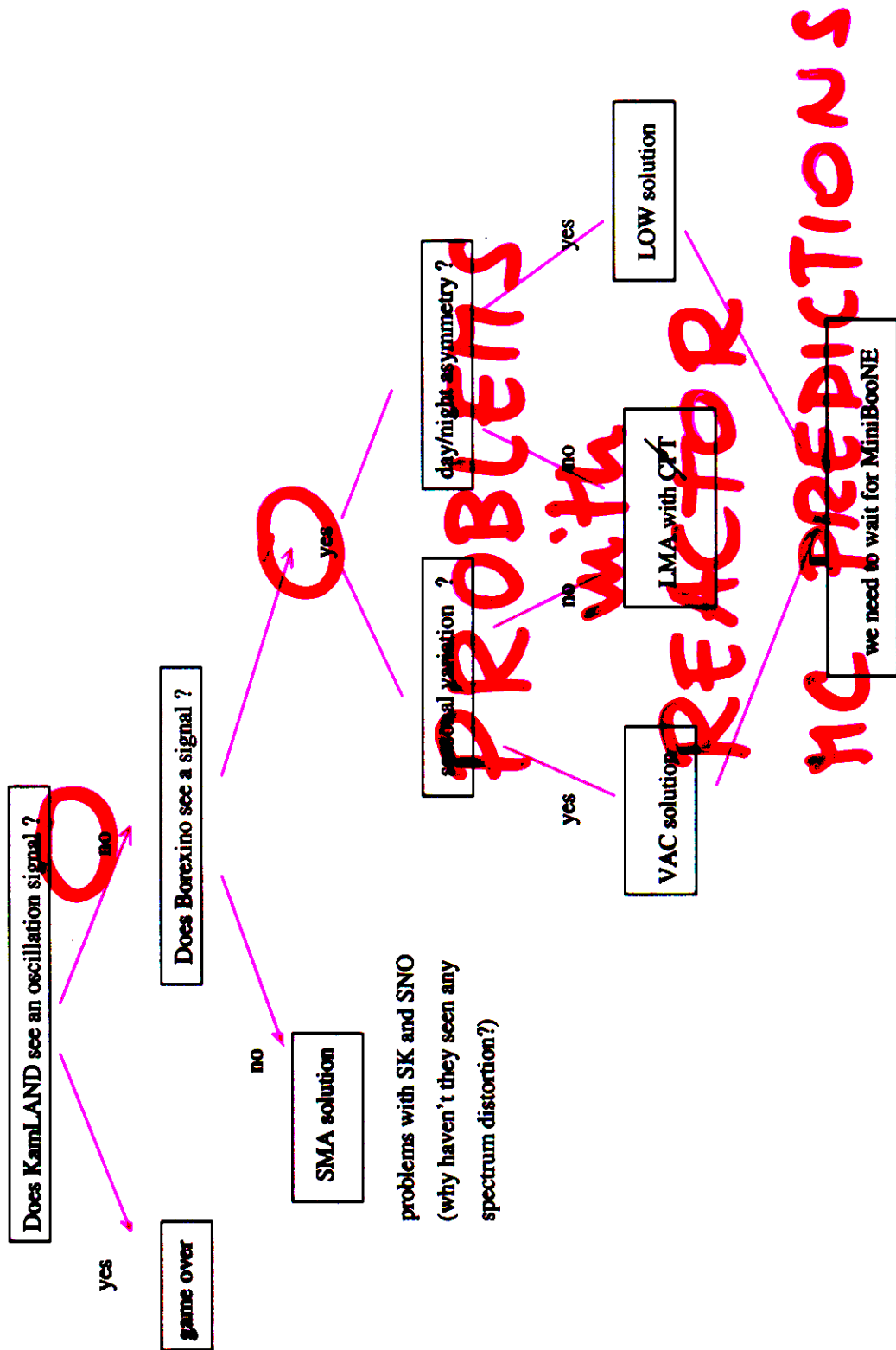


Figure 1: Flow chart for discovering  $CPT$  violation by combining the results of KamLAND and Borexino

hep-ph/0201080

$$P(\nu_e \rightarrow \nu_s) = 0.21 \pm 0.07$$

hep-ph/0202152  
16 February 2002

## $\nu_e \rightarrow \nu_s$ oscillations with large neutrino mass in NuTeV?

Carlo Giunti  
*INFN, Sezione di Torino,*  
and

*Dipartimento di Fisica Teorica, Università di Torino,*  
*Via P. Giuria 1, I-10125 Torino, Italy*

Marco Laveder  
*Dipartimento di Fisica "G. Galilei", Università di Padova,*  
and  
*INFN, Sezione di Padova,*  
*Via F. Marzolo 8, I-35131 Padova, Italy*

### Abstract

We propose an explanation of the NuTeV anomaly in terms of oscillations of electron neutrinos into sterile neutrinos. We derive an average transition probability  $P_{\nu_e \rightarrow \nu_s} \simeq 0.21 \pm 0.07$ , which is compatible with other neutrino data if the mass-squared difference that drives the oscillations is  $\Delta m^2 \sim 10 - 100 \text{ eV}^2$ .

The NuTeV collaboration measured recently [1] a value of the electroweak parameter  $\sin^2 \theta_W$  higher than the standard model prediction obtained from a fit of other electroweak data by

$$\sin^2 \theta_W^{\text{NuTeV}} - \sin^2 \theta_W = (5.0 \pm 1.6) \times 10^{-3}. \quad (1)$$

In this paper we propose an explanation of this discrepancy in terms of  $\nu_e \rightarrow \nu_s$  oscillations<sup>1</sup>, where  $\nu_s$  is a sterile neutrino that does not participate to weak interactions (see [3, 4]). Our analysis is approximate and based on the limited information contained in the paper of the NuTeV collaboration [1]. A precise analysis of NuTeV data in terms of neutrino oscillations can be done only by the NuTeV collaboration.

The NuTeV collaboration measured the ratio of neutral current to charged current cross sections for neutrino scattering with isoscalar targets of  $u$  and  $d$  quarks

$$R^\nu = \frac{\sigma(\nu_\mu + N \rightarrow \nu + X)}{\sigma(\nu_\mu + N \rightarrow \mu^- + X)}, \quad (2)$$

and the corresponding ratio  $R^\bar{\nu}$  for antineutrinos. The Paschos-Wolfenstein relation [5] allows to derive the value of  $\sin^2 \theta_W$  from  $R^\nu$  and  $R^\bar{\nu}$ :

$$\sin^2 \theta_W = \frac{1}{2} - \frac{R^\nu - r R^\bar{\nu}}{1 - r}, \quad (3)$$

<sup>1</sup> Other possible explanations of the NuTeV anomaly have been discussed in Ref. [2].

$\Rightarrow$  REACTOR  $\mu C$  are off by 20%

# TENTATIVE SUMMARY (2002)

## $\nu$ OSCILLATIONS

→ ACTIVE - ACTIVE ( $3\nu$ )  
(LSND missing)

→ ACTIVE - STERILE ( $3\nu$ )  
(SNO disfavored)

→  $4\nu$  MIXING  
(3 active + 1 sterile)

→  $(3 + \bar{3})$  MIXING (CPT)

## $\nu$ OSCILLATIONS + NEW PHYSICS

- $\nu$  DECAY ( $\nu_0$ )
- ANOMALOUS  $\mu$  decay (LSND)
- FCNC
- new  $\nu$  interactions

$\nu$   
M  
I  
X  
I  
N  
G  
?

# CONCLUSIONS

## Oscillation of Solar Neutrinos

### The SNO/SK result

For a long time neutrino oscillations (Bruno Pontecorvo) were suspected to be the cause of the solar neutrino deficit. Now we know!

A combination of the Charged Current measurement presented by SNO and the Neutrino-Electron scattering measurements at SuperKamiokande demonstrates (to  $3\sigma$ ) that the solar neutrino deficit in the high energy part of the spectrum is due to the transformation of electron neutrinos into other active neutrinos, presumably a combination of  $\nu_\mu, \nu_\tau$ .

This result is a real milestone and opens the way for a detailed exploration of the neutrino mixing matrix and mass spectrum, which will occupy our community in the next decades.